

## Stereoregular Oligomers of Methyl Methacrylate: X-Ray Crystal Structure Analysis and $^1\text{H}$ NMR Spectrum of the Trimer

Koichi UTE, Tohru NISHIMURA, Yoshiki MATSUURA,\*  
and Koichi HATADA

Department of Chemistry, Faculty of Engineering Science,  
Osaka University, Toyonaka, Osaka 560, Japan

\* Institute for Protein Research, Osaka University,  
Suita, Osaka 565, Japan

(Received September 22, 1988)

**ABSTRACT:** A trimer of methyl methacrylate was isolated by HPLC from the oligomer mixture prepared in toluene with *t*-BuMgBr, and the crystal and molecular structure was determined by single crystal X-ray analysis. A monoclinic crystal of the trimer grown from heptane belonged to the space group  $P2_1/n$  having cell constants  $a = 10.047$ ,  $b = 24.743$ ,  $c = 9.026$  Å and  $\beta = 109.02^\circ$ . The final  $R$  value was 0.050. The configuration of the trimer was proved to be *meso-meso*. This trimer had been differently assigned to *meso-racemo* isomer in our previous report [K. Hatada *et al.*, *Polym. J.*, **19**, 1325 (1987)]. The conformation in the crystal is  $ttg^+tg^+$  (as (*R,S,R*)-isomer) along the main chain skeletal sequence *t*-Bu-CCCCC- $\text{H}_\omega$ . However, the more extended state  $ttttg^+$  was found to be predominant in solution, from the considerations of the chemical shifts of the methylene protons,  $^4J$ -correlation peaks observed in  $^1\text{H}$  COSY spectrum, and  $^3J$  vicinal coupling constants between the methine and methylene protons in the  $\omega$ -end unit. The chemical shift between the nonequivalent methylene protons in the  $\omega$ -end unit is larger for *racemo*-sequence than for *meso*-sequence, while the opposite is true for in-chain monomeric units.

**KEY WORDS** Methyl Methacrylate / Oligomer / X-Ray Crystal Structure Analysis /  $^1\text{H}$  NMR Spectroscopy / 2D NMR / Conformation / Configuration /  $\alpha$ -End and  $\omega$ -End / Poly(methyl methacrylate) /

Polymerization of methyl methacrylate (MMA) initiated with *t*-BuMgBr in toluene proceeds in a living manner, and highly isotactic PMMA with narrow molecular weight distribution is produced<sup>1,2</sup>. When the living polymerization is terminated by adding methanol to the polymerization mixture, the resulting polymer molecule has a *t*-Bu group at its  $\alpha$ -end and a methine hydrogen at its  $\omega$ -end. The analysis of chain-end structures of the PMMA by two-dimensional NMR spectroscopy<sup>3</sup> revealed that the reaction of the unimer anion with the monomer is less isotactic specific than that of the higher propagating anion with the monomer, and that the reaction of the living PMMA anion with methanol is almost non-stereospecific. Hatada *et al.*<sup>4</sup> also investigated

the initial stage of the polymerization reaction through the structural analysis of the oligomeric products by HPLC and  $^1\text{H}$  NMR spectroscopy.  $^1\text{H}$  NMR spectra of MMA-dimers and trimers prepared by  $\text{CH}_3\text{ONa}$  initiation were reported by Fujishige<sup>5</sup> in 1978. In the above literatures,<sup>3-5</sup> the *meso/racemo* assignments of the monomeric sequences in the PMMA and the oligomeric products were made on the basis of the nonequivalency of methylene protons; the chemical shift between the two nonequivalent methylene protons in a given monomeric unit should be larger for *meso* (*m*) sequences than for *racemo* (*r*) sequences. This nonequivalency was successfully adopted for the interpretation of the  $^1\text{H}$  NMR spectra of the highly isotactic and highly syn-

diotactic PMMAs,<sup>6,7</sup> leading to the first establishment of tacticity determination by NMR spectroscopy. However, there has been doubt as to whether the larger extent of nonequivalency for *meso* methylene protons is held even at the chain-end units. In the present work, this was found not true only for the  $\omega$ -end unit, and the definite *meso/racemo* assignment has been made for the signals of methylene protons at the  $\omega$ -end of chain based on the X-ray analysis of a crystallized trimer.

MMA-oligomers has attracted much attention in terms of the stereochemistry in anionic oligomerizations.<sup>8-10</sup> Moreover, stereoregular oligomers are in themselves good model compounds of stereoregular polymers. The molecular structure of PMMA was investigated by crystallographic studies on isotactic PMMA,<sup>11</sup> wide-range X-ray scattering of syndiotactic PMMA,<sup>12</sup> and conformational energy calculations on the several monomeric sequences embedded in PMMA chains.<sup>13,14</sup> Single crystal structure analysis of the MMA oligomers will provide another approach to the molecular structure of PMMA.

## EXPERIMENTAL

### Preparation of the MMA-trimers

The projection formulae of the MMA-trimers *3mm*, *3mr*, *3rm*, and *3rr* are given in Figure 1. The *3mm* and *3mr* isomers were prepared as reported previously.<sup>4</sup> Polymerization of MMA was initiated with *t*-BuMgBr([MMA]/[*t*-Bu]=50 mol mol<sup>-1</sup>) in toluene at -78°C, and the reaction was terminated 15 min after the initiation by adding a small amount of methanol to the polymerization mixture. The yield of the oligomeric products was 7.5%, and the number average molecular weight  $M_n$  was 470. The oligomer mixture was fractionated by HPLC under the condition described in the literature<sup>9</sup> (on a column packed with silica gel (0.46 (i.d.) × 25 cm) using butyl chloride-acetonitrile (97.5:2.5) as an eluent). Figure 2a

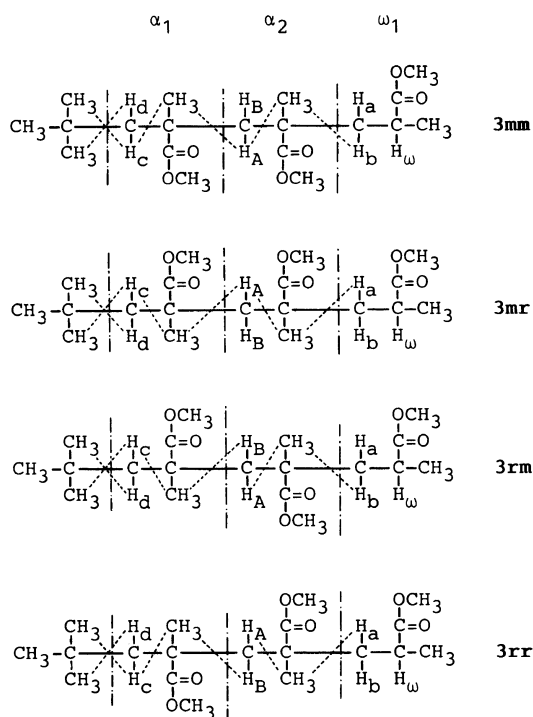


**Figure 1.** The projected formulae of the MMA-trimers *3mm*, *3mr*, *3rm*, and *3rr* (in *tttg*<sup>+</sup> state). Pairs of hydrogen atoms which showed <sup>4</sup>*J* correlation peaks in <sup>1</sup>H COSY spectra due to four-bond planar “W” pathways are connected with dashed lines.

shows the elution curve of the trimer fraction. The diastereomer ratio for the trimers were *mm/mr/rm/rr*=43/52/3/2 by <sup>1</sup>H NMR spectroscopy.<sup>4</sup> Crystals of *3mm* were grown from the heptane solution of the fraction *3mm*+*3rm* (*3mm*/*3rm*=48/3), and one of them was subjected to the X-ray structure analysis. *3rm* and *3rr* were isolated by HPLC from the oligomer mixture ( $M_n$ =570, yield =93%) prepared with *t*-BuLi/Et<sub>3</sub>Al ([Al]/[Li]=2/1 mol mol<sup>-1</sup>, [MMA]/[*t*-Bu]=5 mol mol<sup>-1</sup> in toluene at -78°C<sup>15</sup> (Figure 2b). The diastereomer ratio for the trimer fraction was *mm/mr/rm/rr*=0/1/29/70.

### X-ray Structure Determination of *3mm*

Crystallographic details are given in Table I. The space group was determined unique-

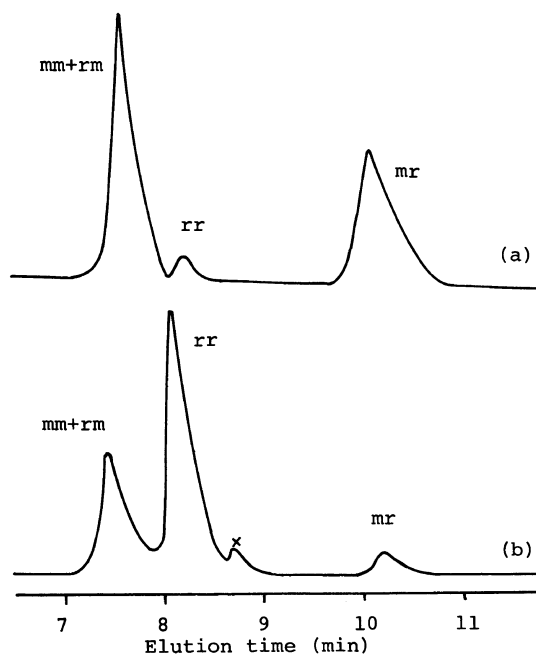


**Figure 2.** The elution curves of the trimer fraction of the oligomer mixture prepared with *t*-BuMgBr (a) and *t*-BuLi/Et<sub>3</sub>Al (b) in toluene at  $-78^\circ\text{C}$ .

ly based on the systematic extinctions:  $h+l=2n+1$  or  $h0l$ ,  $h=2n+1$  for  $h00$ ,  $k=2n+1$  for  $0k0$  and  $l=2n+1$  for  $00l$ . Unit cell parameters were derived from a least-squares calculation based on 20 intense reflections whose  $2\theta$  angles fell in the range of  $44\text{--}46^\circ$ . Three standard reflections monitored every 100 reflections during data collection indicated no appreciable decay. No absorption correction was made.

The structure was solved by the direct method using MULTAN 78.<sup>16</sup> The E map corresponding to the largest combined figure of merit revealed all non-hydrogen atoms. Positions for the non-hydrogen atoms were refined with anisotropic thermal parameters. Difference electron density maps indicated clearly the locations of hydrogen atoms. The final fractional coordinates and thermal parameters for all the atoms appear in Tables II and III.

**Table I.** Crystal data and relevant diffraction data for  $3mm$

Mol formula	$\text{C}_{19}\text{H}_{34}\text{O}_6$
Mol wt.	358.48
Recrystallized solvent	Heptane
Crystal system	Monoclinic
Space group	$\text{P}2_1/n$
$a/\text{\AA}$	10.146
$b/\text{\AA}$	24.742
$c/\text{\AA}$	9.025
$\beta/\text{deg}$	109.02
$V/\text{\AA}^3$	2121.1
$Z$	4
$D_{\text{calcd}}/\text{g cm}^{-3}$	1.123
$\mu(\text{CuK}\alpha)/\text{cm}^{-1}$	6.4
Crystal size/mm	$0.3 \times 0.2 \times 0.2$
Diffractometer	Rigaku AFC5R
$\lambda(\text{CuK}\alpha)/\text{\AA}$	1.5418
$\omega/2\theta$ scan	$1.0 + 0.15 \tan \theta$
Scan speed/ $\text{deg min}^{-1}$	4
$2\theta_{\text{max}}/\text{deg}$	125
Octants measured	$hkl, -hkl$
Total unique data	3390
Obsd. data ( $I > 3\sigma(F)$ )	2718
No. of parameters	362
Max $\Delta/\sigma$ in final cycle	0.159
$R^a$	0.050
$R_w^b$	0.052
Goodness of fit <sup>c</sup>	1.47

$$^a R = \sum \|F_o\| - |F_c| / \sum \|F_o\|$$

$$^b R_w = [\sum w(|F_o| - |F_c|)^2 / \sum w |F_o|^2]^{1/2}; w = 1/\sigma^2(|F_o|)$$

$$^c \text{g.o.f} = [\sum w(|F_o| - |F_c|)^2 / (N_{\text{obsd}} - N_{\text{parms}})]^{1/2}$$

### $^1\text{H}$ NMR Measurements

$^1\text{H}$  NMR spectra were measured in  $\text{CDCl}_3$  at  $35^\circ\text{C}$  using a JEOL JNM-GX500 spectrometer (500 MHz).  $^1\text{H}$  COSY experiments on the trimers were performed with the standard  $90^\circ\text{-}t_1\text{-}90^\circ\text{-}t_2$  pulse sequence. A recycle time of 2.5 s was employed, and 8 transients were accumulated for each  $t_1$  value. A total of 512 spectra, each consisting of 1024 data points were collected with a frequency range of 1600 Hz in both dimensions.

## RESULTS AND DISCUSSION

### X-Ray Crystal Structure Analysis of $3mm$

Figure 3 shows the ORTEP drawing of  $3mm$ . Crystal symmetry demands the crystal

**Table II.** Fractional atomic coordinates ( $\times 10^4$ ) and equivalent isotropic thermal parameters ( $\times 10^3$ ) for  $3mm$ 

Atom	<i>X/a</i>	<i>Y/b</i>	<i>Z/c</i>	$U_{eq}/\text{\AA}^2$
C1	13714( 5)	3751( 2)	12561( 4)	107( 2)
C2	12747( 4)	4620( 2)	11333( 5)	96( 2)
C3	14546( 4)	4124( 2)	10487( 5)	115( 3)
C4	13267( 2)	4069( 1)	10998( 3)	60( 1)
C5	12112( 2)	3713( 1)	9849( 3)	54( 1)
C6	11194( 2)	3889( 1)	8163( 2)	44( 1)
C7	10151( 3)	4336( 1)	8195( 3)	54( 1)
C8	12171( 2)	4044( 1)	7257( 2)	47( 1)
C9	12972( 5)	4728( 2)	5935( 6)	93( 2)
C10	10415( 2)	3356( 1)	7428( 3)	46( 1)
C11	9196( 2)	3365( 1)	5837( 2)	46( 1)
C12	8839( 3)	2766( 1)	5400( 3)	62( 1)
C13	7876( 2)	3622( 1)	6006( 3)	51( 1)
C14	6206( 3)	3587( 2)	7345( 5)	87( 2)
C15	9607( 2)	3660( 1)	4551( 3)	51( 1)
C16	8606( 2)	3597( 1)	2861( 3)	53( 1)
C17	8676( 4)	4100( 1)	1889( 3)	71( 2)
C18	8965( 3)	3119( 1)	2044( 3)	57( 1)
C19	8081( 4)	2457( 1)	77( 4)	81( 2)
O1	12969( 2)	3736( 1)	6945( 2)	62( 1)
O2	12074( 2)	4565( 1)	6834( 2)	63( 1)
O3	7219( 2)	3985( 1)	5219( 2)	67( 1)
O4	7488( 2)	3391( 1)	7133( 2)	70( 1)
O5	10127( 2)	2958( 1)	2219( 2)	93( 1)
O6	7827( 2)	2899( 1)	1010( 2)	72( 1)
H1	14372(34)	3489(13)	12143(38)	79(12)
H2	12668(50)	3795(18)	12942(54)	154(19)
H3	14428(35)	3954(13)	13360(42)	81(11)
H4	12624(40)	4873(16)	10362(50)	117(17)
H5	11866(42)	4610(14)	11714(45)	106(15)
H6	13445(34)	4799(12)	12227(41)	77(10)
H7	14073(29)	4508(11)	9878(38)	48(9)
H8	15347(33)	4327(12)	11380(40)	83(10)
H9	14582(39)	4216(16)	9491(49)	95(14)
H10	12597(22)	3367( 9)	9701(26)	28( 6)
H11	11353(25)	3637( 9)	10393(29)	39( 7)
H12	9573(26)	4201(10)	8787(30)	42( 8)
H13	9572(23)	4433( 9)	7071(29)	31( 6)
H14	10620(23)	4658( 9)	8714(27)	28( 6)
H15	12726(38)	4545(15)	4957(48)	100(15)
H16	12826(37)	5111(17)	5716(45)	106(14)
H17	13976(53)	4655(19)	6480(58)	155(24)
H18	11148(21)	3101( 8)	7278(23)	17( 5)
H19	10037(19)	3215( 7)	8203(23)	8( 5)
H20	9618(25)	2577( 9)	5132(28)	34( 7)
H21	7977(28)	2735(10)	4399(34)	52( 8)
H22	8590(25)	2594(10)	6261(31)	40( 8)
H23	5980(35)	3364(13)	8120(43)	89(12)
H24	5485(34)	3615(13)	6344(43)	84(12)
H25	6320(34)	3968(14)	7544(40)	79(14)
H26	10534(23)	3509( 8)	4531(24)	21( 6)

**Table II.** (contd.)

Atom	<i>X/a</i>	<i>Y/b</i>	<i>Z/c</i>	$U_{eq}/\text{\AA}^2$
H27	9691(21)	4079( 9)	4833(25)	22( 6)
H28	7624(24)	3528( 8)	2870(26)	28( 6)
H29	8096(31)	4047(11)	772(38)	66( 9)
H30	9660(33)	4157(11)	1825(35)	66(10)
H31	8383(30)	4436(12)	2397(35)	69(10)
H32	8389(35)	2137(14)	762(44)	91(12)
H33	7182(38)	2402(14)	-747(47)	100(13)
H34	8868(34)	2558(12)	-414(40)	80(12)

<sup>a</sup> Estimated standard deviations are in parentheses.

<sup>b</sup>  $U_{eq} = \sum U_{ij} a_i^* a_j^* a_i a_j$ , where the temperature factors are defined as  $\exp(-2\pi^2 \sum h_i h_j a_i^* a_j^* U_{ij})$ .

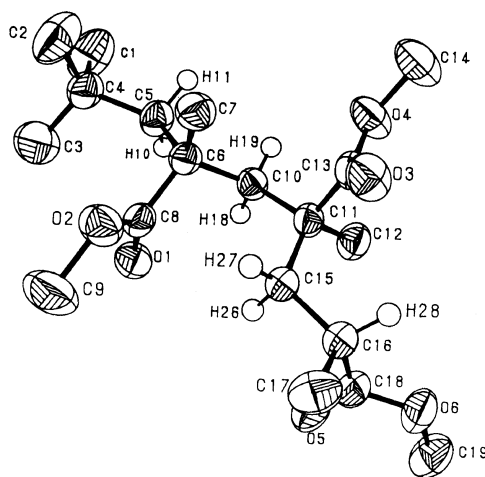


**Figure 3.** The ORTEP drawing of  $3mm$  ((*R,S,R*)-form). Methyl hydrogen atoms are omitted in this figure. The numbering for methyl hydrogens are as follows: H1–H3(C1); H4–H6(C2), H7–H9(C3), H12–H14(C7), H15–H17(C9), H20–H22(C12), H23–H25(C14), H29–H31(C17), H32–H34(C19).

consisting of a racemic mixture of the (*R,S,R*) and (*S,R,S*) isomers. Only the (*R,S,R*) configuration of the quaternary carbons (C6, C11, C16) is shown in the figure. All the atomic parameters and torsional angles in the present work are given in the (*R,S,R*) form. Repetition of the three monomeric units ( $\alpha_1, \alpha_2, \omega_1$ ) in the (*R,S,R*) form between C5 and C16 produces an isotactic PMMA chain, and therefore the trimer is assigned to the *meso-meso* (*mm*) diastereomer. This trimer was differently assigned

**Table III.** Anisotropic thermal parameters<sup>a</sup> ( $\times 10^3$ ) for *3mm*

	$U_{11}$	$U_{22}$	$U_{33}$	$U_{12}$	$U_{23}$	$U_{13}$
C1	113(3)	117(3)	55(2)	-3(2)	-23(2)	-1(2)
C2	86(2)	92(3)	87(3)	-2(2)	-5(2)	-35(2)
C3	56(2)	209(5)	72(2)	-39(3)	11(2)	-35(3)
C4	50(1)	73(2)	47(1)	-2(1)	3(1)	-6(1)
C5	51(1)	62(2)	42(1)	-1(1)	4(1)	2(1)
C6	39(1)	51(1)	38(1)	2(1)	8(1)	1(1)
C7	49(1)	61(2)	51(1)	5(1)	15(1)	-3(1)
C8	41(1)	54(1)	43(1)	-3(1)	8(1)	-7(1)
C9	126(3)	81(2)	101(3)	-19(2)	75(3)	6(2)
C10	41(1)	53(1)	42(1)	-2(1)	10(1)	4(1)
C11	39(1)	53(1)	42(1)	-5(1)	8(1)	1(1)
C12	66(2)	60(2)	57(2)	-13(1)	13(1)	-4(1)
C13	40(1)	64(1)	44(1)	-8(1)	6(1)	3(1)
C14	56(2)	129(4)	86(2)	15(2)	36(2)	24(2)
C15	45(1)	65(2)	41(1)	-7(1)	11(1)	-2(1)
C16	45(1)	69(2)	42(1)	-5(1)	10(1)	0(1)
C17	86(2)	73(2)	52(2)	6(2)	21(2)	10(1)
C18	54(1)	69(2)	42(1)	-5(1)	5(1)	3(1)
C19	102(3)	66(2)	63(2)	-14(2)	11(2)	-13(2)
O1	51(1)	69(1)	73(1)	1(1)	27(1)	-11(1)
O2	73(1)	54(1)	69(1)	-5(1)	34(1)	3(1)
O3	53(1)	79(1)	64(1)	11(1)	14(1)	19(1)
O4	49(1)	101(1)	66(1)	8(1)	26(1)	27(1)
O5	61(1)	121(2)	85(1)	12(1)	6(1)	-36(1)
O6	65(1)	77(1)	60(1)	-13(1)	1(1)	-9(1)

<sup>a</sup> Estimated standard deviations are given in parentheses. The anisotropic temperature factors are defined as  $\exp(-2\pi^2 \sum h_i h_j a_i^* a_j^* U_{ij})$ .

to the *meso-racemo* (*mr*) diastereomer in our previous reports.<sup>3,4</sup>

The conformation of the main chain is *ttg*<sup>+</sup>*tg*<sup>+</sup> along the skeletal sequence C4-C5-C6-C10-C11-C15-C16-H28 (Table IV). All the ester groups take planar *S-cis* conformation. The plane of the ester group of  $\alpha_1$  unit (O1=C8-O2-C9) occurs approximately perpendicular to the plane defined by the adjoining skeletal bonds (C5-C6-C10), with the carbonyl group oriented to the opposite side (*anti*) of the  $\alpha$ -methyl carbon (C7). The plane of the ester group of  $\alpha_2$  unit (O3=C13-O4-C14) appreciably deviated from perpendicular to the plane defined by the adjoining skeletal bonds (C10-C11-C15) which is in a *tg*<sup>+</sup> state. The *interdyad* bond angles CH<sub>2</sub>-C-CH<sub>2</sub> are 103.5° for C5-C6-C10 in a *tt* state, and 112.3° for C10-C11-C15 in a *tg*<sup>+</sup> state, which agree

well with the values calculated by conformational statistics for four-bond segments embedded in PMMA chains.<sup>13</sup> The unusually large values for the *intradymad* bond angles C-CH<sub>2</sub>-C, which were described in the literatures,<sup>11-14</sup> are also observed (Table IV). Bond lengths and bond angles for side chains show little difference among the three monomeric units. These structural parameters will support the conformational analysis of PMMA. The authors are presently trying to crystallize the remaining three isomers *3mr*, *3rm*, and *3rr*, and oligomers of the higher degree of polymerization.

#### <sup>1</sup>H NMR Spectra of the MMA Trimers *3mm*, *3mr*, *3rm* and *3rr*

Figure 4 shows <sup>1</sup>H NMR spectra of the MMA trimers *3mm*, *3mr*, *3rm*, and *3rr*. The

**Table IV.** Selected bond lengths, angles and torsional angles for  $3mm^a$ 

Monomeric units					
$\alpha_1$		$\alpha_2$		$\omega_1$	
Bond lengths/Å					
C4-C5	1.554	C10-C11	1.554	C15-C16	1.538
C5-C6	1.562	C11-C12	1.546	C16-C17	1.538
C6-C7	1.532	C11-C13	1.523	C16-C18	1.498
C6-C8	1.517	C11-C15	1.537	C16-H28	1.003
C6-C10	1.565	C13-O3	1.201	C18-O5	1.195
C8-O1	1.204	C13-O4	1.332	C18-O6	1.333
C8-O2	1.339	C14-O4	1.447	C19-O6	1.452
C9-O2	1.453				
Bond angles (deg)					
C4-C5-C6	124.6	C6-C10-C11	121.0	C11-C15-C16	116.8
C5-C6-C10	103.5	C10-C11-C15	112.3	C15-C16-H28	109.6
C7-C6-C8	113.2	C12-C11-C13	106.8	C17-C16-C18	107.2
C6-C8-O2	113.4	C11-C13-O4	112.2	C16-C18-O6	112.2
O1-C8-O2	122.4	O3-C13-O4	122.2	O5-C18-O6	122.3
C8-O2-C9	115.1	C13-O4-C14	116.8	C18-O6-C19	116.2
Torsional angles (deg)					
C4-C5-C6-C10	170.4	C6-C10-C11-C15	51.4	C11-C15-C16-H28	27.6
C5-C6-C10-C11	169.9	C10-C11-C15-C16	168.1		
C7-C6-C8-O1	-171.9	C12-C11-C13-O3	-117.7	C17-C16-C18-O5	86.3
O1-C8-O2-C9	1.6	O3-C13-O4-C14	1.6	O5-C18-O6-C19	-1.2
				H26-C15-C16-H28	147.5
				H27-C15-C16-H28	-93.8

<sup>a</sup> The estimated standard deviations for bond lengths, bond angles and torsional angles involving only non-hydrogen atoms are 0.003–0.005 Å, 0.2–0.3 deg and 0.2–0.4 deg, respectively.

assignments for the  $^1\text{H}$  NMR signals in these spectra were unambiguously made by two-dimensional NMR spectroscopy. Figure 5 displays the  $^1\text{H}$  COSY spectrum of  $3mm$  (refer to Figure 1 for the notation of the individual protons). Starting from the strong singlet at 0.89 ppm due to *t*-Bu protons, we can identify the signals of  $\text{H}_d$ ,  $\text{H}_c$ ,  $\text{CH}_3(\alpha_1)$ ,  $\text{H}_A$ ,  $\text{CH}_3(\alpha_2)$ , and  $\text{H}_b$  successively by the correlation peaks 1 to 6 in Figure 5 due to  $^4J$  long range coupling. It should be noted that correlation peaks due to  $^4J$  long range coupling were not or very weakly observed between the signals of  $\text{CH}_3(\alpha_1)$  and  $\text{H}_B$ ,  $\text{H}_B$  and  $\text{CH}_3(\alpha_2)$ ,  $\text{CH}_3(\alpha_2)$  and  $\text{H}_a$ ,  $\text{H}_a$  and  $\text{CH}_3(\omega_1)$ , and  $\text{H}_b$  and  $\text{CH}_3(\omega_1)$ ; as will be discussed later, intensities of the  $^4J$  correlation peaks are sensitive to the conformation of the trimers. The signal as-

signment for  $\text{H}_B$  and  $\text{H}_a$  can be made from the correlation peaks with the signals of  $\text{H}_A$  and  $\text{H}_b$  (correlation peaks 8 and 9), respectively, due to  $^2J$  geminal coupling.  $^2J$  correlation peaks also appeared between the signals of  $\text{H}_c$  and  $\text{H}_d$  (correlation peak 7). The signals of  $\text{H}_a$  and  $\text{H}_b$  showed connectivity with  $\text{H}_\omega$  (correlation peaks 10 and 11), and the signal of  $\text{H}_\omega$  with  $\text{CH}_3(\omega_1)$  (correlation peak 12), owing to  $^3J$  vicinal coupling. In this way, assignments for  $^1\text{H}$  NMR signals due to all but  $\text{OCH}_3$  protons were achieved. The  $^1\text{H}$  NMR assignments for  $3mr$ ,  $3rm$ , and  $3rr$  were carried out in a similar manner.<sup>17</sup>

The configuration of the in-chain monomeric sequence of  $3mm$  and  $3mr$  should be *meso*, since  $3mm$  and  $3mr$  are the predominant trimers isolated from the mixture of highly

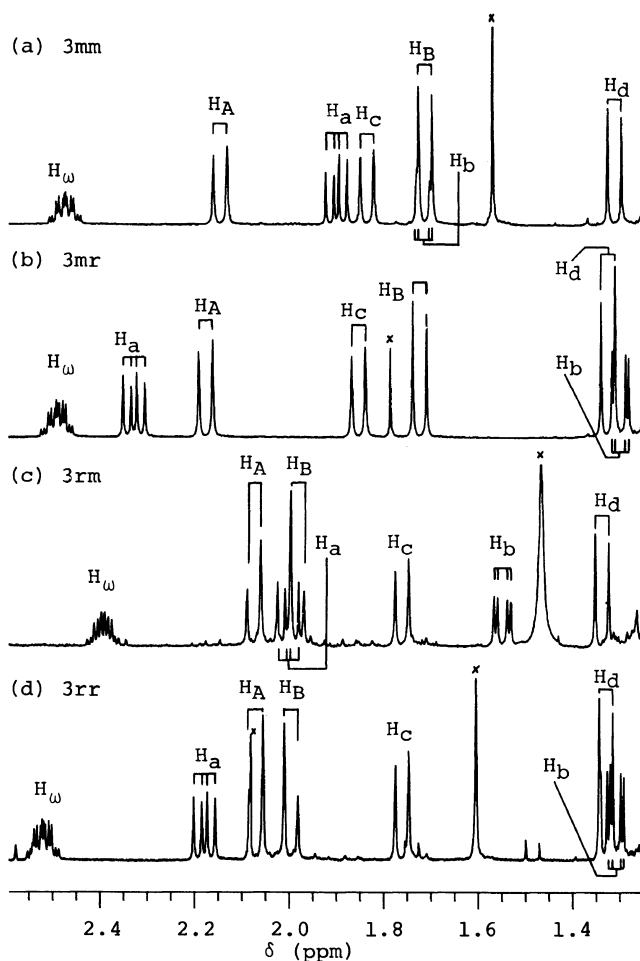


**Figure 4.**  $^1\text{H}$  NMR spectra (methine and methylene protons region) of  $3mm$  (a),  $3mr$  (b),  $3rm$  (c), and  $3rr$  (d) measured in  $\text{CDCl}_3$  at  $35^\circ\text{C}$  and at 500 MHz.

isotactic oligomers prepared with  $t\text{-BuMgBr}$ . The comparable yields of the  $\omega$ -*meso* ( $3mm$ ) and the  $\omega$ -*racemo* ( $3mr$ ) isomers resulted from the non-stereospecific reaction of the isotactic-specific anion with the protonating reagent (methanol). The  $^1\text{H}$  NMR spectrum of  $3mm$  (Figure 4a), whose structure is now confirmed by the X-ray single crystal analysis, and the spectrum of the other isomer  $3mr$  (Figure 4b) clearly indicate that the chemical shift between the methylene protons in the  $\omega$ -end ( $\omega_1$ ) unit ( $\text{H}_a$  and  $\text{H}_b$ ) is smaller for  $m$ -sequence than for  $r$ -sequence. On the other hand, the chemical

shift between the methylene protons in the in-chain ( $\alpha_2$ ) unit ( $\text{H}_A$  and  $\text{H}_B$ ) is larger for  $m$ -sequences of  $3mm$  and  $3mr$  than for  $r$ -sequences of  $3rm$  and  $3rr$ , the predominant trimers isolated from the highly syndiotactic oligomers prepared with  $t\text{-BuLi}/\text{Et}_3\text{Al}$  complex (Figures 4c and 4d). The chemical shifts between the nonequivalent methylene protons of the trimers ( $\text{H}_A$  and  $\text{H}_B$ ,  $\text{H}_a$  and  $\text{H}_b$ ) are summarized in Table V.

The  $ttg^+tg^+$  form, the conformation which  $3mm$  adopts in its crystal, accounts for the small extent of nonequivalency between  $\text{H}_a$

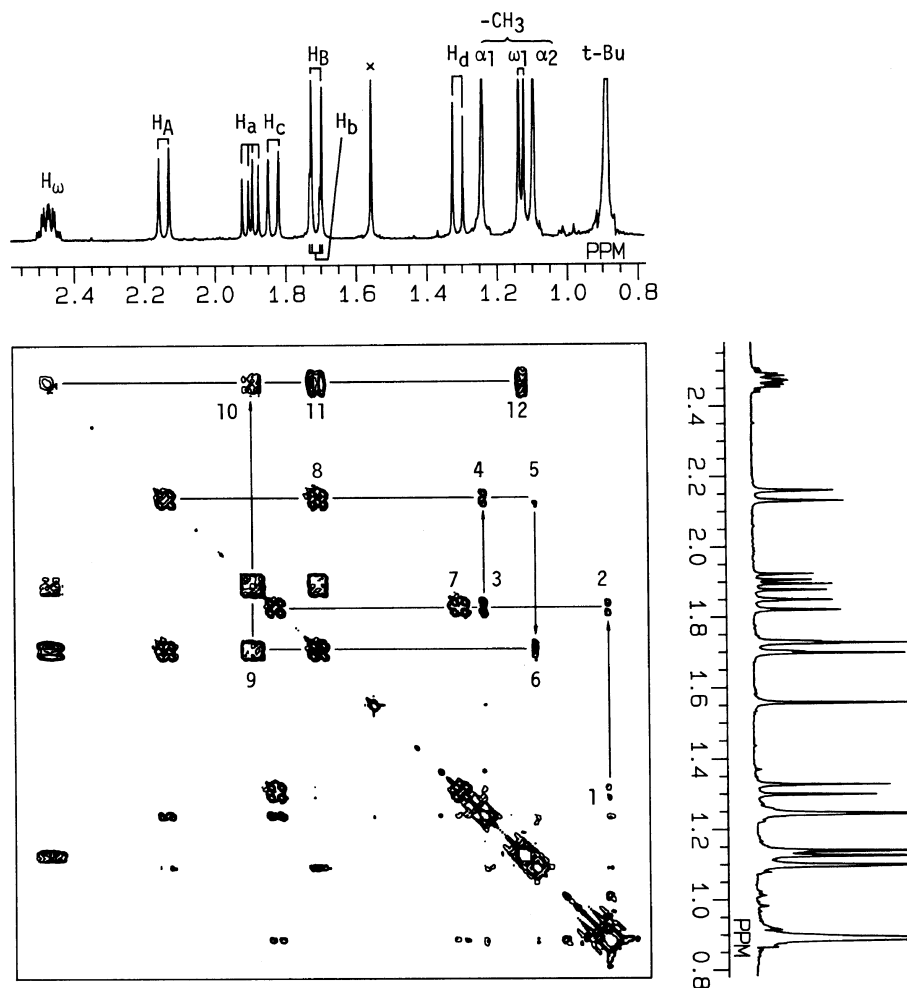


Figure 5. 500 MHz  $^1\text{H}$  COSY spectrum of  $3\text{mm}$  in  $\text{CDCl}_3$  at  $35^\circ\text{C}$ . Correlation peaks numbered as 1 to 6, 7 to 9 and 10 to 12 are due to  $^4J$  long range,  $^2J$  geminal, and  $^3J$  vicinal couplings, respectively.

and  $\text{H}_b$ , but does not for the large extent of nonequivalency between  $\text{H}_A$  and  $\text{H}_B$ ; it would be realized from Figure 3 that magnetic environment is quite similar for  $\text{H}_A$  (H18) and  $\text{H}_B$  (H19). The nonequivalencies of the methylene protons in in-chain and  $\omega$ -end units of the trimers can be explained if we assume the more extended,  $\text{ttttg}^+$  form in solution for the main chains of all the four trimers (Figure 1); in the  $\omega$ -*racemo* units,  $\text{H}_a$  is flanked by carbonyl groups on both sides analogously to  $\text{H}_A$  in in-chain *meso* units and  $\text{H}_b$  is flanked by no

carbonyl group analogously to  $\text{H}_B$  in in-chain *meso* units, whereas in the  $\omega$ -*meso* units,  $\text{H}_a$  and  $\text{H}_b$  are both flanked by a carbonyl group only on the side analogously to  $\text{H}_A$  and  $\text{H}_B$  in in-chain *racemo* units.

Predominance of  $\text{ttttg}^+$  form in solution was further evidenced from  $^4J$  long range coupling. As mentioned previously, correlation peaks due to  $^4J$  long range coupling with  $\alpha$ - $\text{CH}_3$  protons appeared only in one of the two nonequivalent methylene protons. This indicates the existence of four-bond planar "W"



**Table V.** The chemical shifts between the methylene protons in  $\alpha_2$  units ( $\text{H}_\text{A}$ ,  $\text{H}_\text{B}$ ) and  $\omega_1$  units ( $\text{H}_\text{a}$ ,  $\text{H}_\text{b}$ ) and the  $^3J_{\text{HH}}$  vicinal coupling constants between the  $\omega$ -end methine proton ( $\text{H}_\omega$ ) and  $\text{H}_\text{a}$ ,  $\text{H}_\text{b}$  for  $3mm$ ,  $3mr$ ,  $3rm$ , and  $3rr^a$

	$3mm$	$3mr$	$3rm$	$3rr$
$\delta(\text{H}_\text{A}) - \delta(\text{H}_\text{B})/\text{ppm}$	0.43	0.45	0.07	0.09
$\delta(\text{H}_\text{a}) - \delta(\text{H}_\text{b})/\text{ppm}$	0.19	1.03	0.45	0.87
$^3J(\text{H}_\text{a} - \text{H}_\omega)/\text{Hz}$	8.7	8.6	8.1	8.5
$^3J(\text{H}_\text{b} - \text{H}_\omega)/\text{Hz}$	2.4	3.2	3.9	3.2

<sup>a</sup> In  $\text{CDCl}_3$  at  $35^\circ\text{C}$ .

pathways between the respective protons in a highly preferred conformation of the MMA units. The four-bond planar "W" pathways of  $\text{CH}_2\text{-C-CH}_3$  protons require that one of the methylene protons and the methyl carbon should be in *trans* ( $t$ ) state. Thus  $\text{H}_\text{c}$  and  $\text{CH}_3(\alpha_1)$ ,  $\text{CH}_3(\alpha_1)$  and  $\text{H}_\text{A}$ ,  $\text{H}_\text{A}$  and  $\text{CH}_3(\alpha_2)$ , and  $\text{CH}_3(\alpha_2)$  and  $\text{H}_\text{b}$  of  $3mm$  should be in *trans* state, respectively, and neither of  $\text{H}_\text{a}$  and  $\text{H}_\text{b}$  can be *trans* to  $\text{CH}_3(\omega_1)$ . These considerations are completely satisfied with  $tttg^+$  form of  $3mm$ .  $^1\text{H}$  COSY spectra of the other trimers suggested that  $3mr$ ,  $3rm$ , and  $3rr$  also adopt  $tttg^+$  conformations in solution<sup>17</sup>. The  $^4J$  connectivities observed in the  $^1\text{H}$  COSY spectra are shown with dashed lines in Figure 1. Similar  $^4J$  connectivities were reported in isotactic PMMA<sup>18</sup> and the related compounds<sup>19</sup>.

The  $^3J$  vicinal coupling constants between  $\text{H}_\text{a}$  and  $\text{H}_\omega$ , and between  $\text{H}_\text{b}$  and  $\text{H}_\omega$  in the trimers are 8.1–8.7, and 2.4–3.9 Hz, respectively (Table V), suggesting that  $\text{H}_\text{a}$  and  $\text{H}_\omega$  are in nearly *trans* ( $t$ ) state, and  $\text{H}_\text{b}$  and  $\text{H}_\omega$  are in nearly *gauche* ( $g^-$ ) state. Therefore the conformation of the  $\omega$ -end skeletal sequence  $\text{C-CH}_2\text{-C-H}_\omega$  should be  $g^+$  form for all the trimers in solution. The conformational energy calculations for the *meso* and *racemo* dimers also support the  $g^+$  conformation of the  $\omega$ -ends.<sup>20</sup>

**Acknowledgments.** The authors are grateful to Mr. K. Sakaguchi (Institute for Protein

Research, Osaka University) for his assistance in the X-ray experiment, and to Dr. H. Imoto (Faculty of Engineering Science, Osaka University) for his help on structural refinement.

A part of this work was supported by a Grant-in-Aid for Scientific Research (No. 6143022) from the Ministry of Education, Science, and Culture of Japan.

**Supplementary Material Available:** Tables of calculated and observed factors for the compound  $3mm$  (13 pages). On request, these materials are available from the authors or editorial office of The Society of Polymer Science, Japan.

## REFERENCES

1. K. Hatada, K. Ute, K. Tanaka, T. Kitayama, and Y. Okamoto, *Polym. J.*, **17**, 977 (1985).
2. K. Hatada, K. Ute, K. Tanaka, Y. Okamoto, and T. Kitayama, *Polym. J.*, **18**, 1037 (1986).
3. K. Hatada, K. Ute, K. Tanaka, M. Imanari, and N. Fujii, *Polym. J.*, **19**, 425 (1987).
4. K. Hatada, K. Ute, K. Tanaka, and T. Kitayama, *Polym. J.*, **19**, 1325 (1987).
5. S. Fujishige, *Makromol Chem.*, **179**, 2251 (1978).
6. F. A. Bovey and G. V. D. Tiers, *J. Polym. Sci.*, **44**, 173 (1960).
7. A. Nishioka, H. Watanabe, K. Abe, and Y. Sono, *J. Polym. Sci.*, **48**, 241 (1960).
8. G. Wulff, R. Sczegan, and A. Steigel, *Tetrahedron Lett.*, **27**, 1991 (1986).
9. Y. Okamoto, E. Yashima, T. Nakano, and K. Hatada, *Chem. Lett.*, 759 (1987).
10. R. A. Volpe, T. E. Hogen-Esch, A. H. E. Muller, and F. Gores, *Polym. Prepr., Am. Chem. Soc. Div. Polym. Chem.*, **28**(2), 423 (1987).
11. H. Kusanagi, H. Tadokoro, and Y. Chatani, *Macromolecules*, **9**, 531 (1976).
12. R. Lovell and A. H. Windle, *Polymer*, **22**, 175 (1981).
13. M. Vacatello and P. J. Flory, *Macromolecules*, **19**, 405 (1986).
14. P. R. Sundararajan, *Macromolecules*, **19**, 415 (1986).
15. T. Kitayama, T. Shinozaki, E. Masuda, M. Yamamoto, and K. Hatada, *Polym. Bull.*, **20**, 505 (1988).
16. P. Main, S. E. Hull, L. Lessinger, G. Germain, J.-P. Declercq, and M. M. Woolfson, A System of Computer Programs for the Automatic Solution of Crystal Structures from X-ray Diffraction Data, University of York.
17. K. Ute, T. Nishimura, and K. Hatada, *Polym. J.*, to be submitted.

18. F. C. Schilling, F. A. Bovey, M. D. Bruch, and S. A. Kozlowski, *Macromolecules*, **18**, 1418 (1985).
19. S. R. Johns, R. I. Willing, and D. A. Winkler, *Makromol. Chem., Rapid Commun.*, **8**, 17 (1987).
20. K. Hatada, K. Ute, T. Nishimura, and K. Tanaka, Presented at the IUPAC 32nd International Symposium on Macromolecules, 4P03a-pm, Kyoto, Japan (1988); K. Ute, T. Nishimura, K. Hatada, Y. Matsuura, and K. Sakaguchi, *Polym. Prepr. Jpn.*, **37**, 2480 (1988).